

## THE RANDOM PROJECTION METHOD FOR STIFF DETONATION CAPTURING\*

WEIZHU BAO<sup>†</sup> AND SHI JIN<sup>‡</sup>

**Abstract.** In this paper we present a simple and robust random projection method for under-resolved numerical simulation of stiff detonation waves in chemically reacting flows. This method is based on the random projection method proposed by the authors for general hyperbolic systems with stiff reaction terms [W. Bao and S. Jin, *J. Comput. Phys.*, 163 (2000), pp. 216–248], where the ignition temperature is randomized in a suitable domain. It is simplified using the equations of instantaneous reaction and then extended to handle the interactions of detonations. Extensive numerical experiments, including interaction of detonation waves, and in two dimensions, demonstrate the reliability and robustness of this novel method.

**Key words.** detonation, random projection method, reacting flow, shock capturing

**AMS subject classifications.** 80A32, 35L67, 65M60

**PII.** S1064827599364969

**1. Introduction.** An inviscid, compressible, reacting flow is described by the reactive Euler equations

$$(1.1) \quad U_t + F(U)_x + G(U)_y = \frac{1}{\varepsilon} \Psi(U),$$

$$(1.2) \quad U = \begin{pmatrix} \rho \\ m \\ n \\ e \\ \rho z \end{pmatrix}, \quad F(U) = \begin{pmatrix} m \\ m^2/\rho + p \\ mn/\rho \\ m(e+p)/\rho \\ mz \end{pmatrix}, \quad G(U) = \begin{pmatrix} n \\ mn/\rho \\ n^2/\rho + p \\ n(e+p)/\rho \\ nz \end{pmatrix},$$

$$(1.3) \quad \Psi(U) = \begin{pmatrix} 0 \\ 0 \\ 0 \\ 0 \\ -\rho z e^{-T_c/T} \end{pmatrix} \equiv \begin{pmatrix} 0 \\ 0 \\ 0 \\ 0 \\ \psi(U) \end{pmatrix}.$$

The dependent variables  $\rho(x, y, t)$ ,  $m(x, y, t)$ ,  $n(x, y, t)$ ,  $e(x, y, t)$ , and  $z(x, y, t)$  are the density,  $x$ - and  $y$ -momentum, total energy, and the fraction of unburnt fluid, respectively. The pressure for ideal gas is given by

$$p = (\gamma - 1) \left( e - \frac{1}{2} (m^2 + n^2) / \rho - q_0 \rho z \right),$$

and the temperature is defined as  $T = p/\rho$ . Let  $(u, v) = (m/\rho, n/\rho)$  be the velocity. The parameters  $q_0$ ,  $T_c$ ,  $\gamma$ , and  $\varepsilon$  correspond to chemical heat release, ignition temperature,  $c_p$  to  $c_v$  ratio, and reaction time, respectively. The equations have been

\*Received by the editors December 16, 1999; accepted for publication (in revised form) March 26, 2001; published electronically September 26, 2001.

<http://www.siam.org/journals/sisc/23-3/36496.html>

<sup>†</sup>Department of Computational Science, National University of Singapore, Singapore 117543 (bao@cz3.nus.edu.sg.)

<sup>‡</sup>Department of Mathematics, University of Wisconsin-Madison, Madison, WI 53706 (jin@math.wisc.edu). This author's research was supported in part by NSF grants DMS-9704957 and DMS-0196106.

nondimensionalized, leaving the choice of these four parameters to completely determine the problem.

The focus of this paper is on the computations of stiff detonation waves. For these waves the viscosity is not as important as for the slower deflagration wave solutions.

Equations (1.1)–(1.3) are usually referred to as the reactive Euler equations with Arrhenius kinetics. When the source term is replaced by

$$-\frac{1}{\varepsilon}\rho z H(T - T_c),$$

where  $H(x) = 1$  for  $x > 0$  and  $H(x) = 0$  for  $x < 0$ , the kinetics is referred to as the *Heaviside kinetics* [21]. The difference in the kinetics affect the details of the detonation layers, which are of width  $O(\varepsilon)$  with pressure and temperature spikes that decay exponentially into the postdetonation equilibria.

One of the main numerical challenges for reacting flows is that the kinetics equations (1.1) often include reactions with widely varying time scales. The chemical time scales, as characterized by  $\varepsilon$ , may be orders of magnitude faster than the fluid dynamical time scale. This leads to problems of severe numerical stiffness. Actually, the stiffness issue with the Heaviside kinetics is the more severe one [11]. Even a stable numerical scheme may lead to spurious unphysical solutions unless the small chemical time scale is fully resolved numerically.

Numerical methods for such problems have attracted a great deal of attention in the last decade. In particular, many works have contributed to the analysis and development of underresolved numerical methods which are capable of capturing the physically relevant macroscopic solutions without resolving the details of the detonation layers. Of course, when one does not resolve the chemical scale numerically (using grid size larger than the reaction zone  $O(\varepsilon)$ ), it is impossible to capture the pressure and temperature spikes in the reaction zone. Thus the best one can hope for is to capture the speed of detonation, as well as other wave features associated with the fluid dynamics. It was first observed by Colella, Majda and Roytburd [9] that an underresolved numerical method, where  $\varepsilon$  is not resolved by suitably small time steps and grid sizes, leads to a spurious weak detonation wave that travels one grid per time step. Since then, lots of attention has been paid to study this peculiar numerical phenomenon (see [4], [6], [13], [18], [19]). It is known that numerical shock profile, an essential ingredient in all shock capturing methods, leads to premature chemical reactions once the smeared value of the temperature in the numerical detonation layer is above the ignition temperature. Various approaches have been suggested to fix this numerical problem. For example, in [11], a temperature extrapolation technique was proposed. In [5] the ignition temperature was artificially raised. In [20] the reaction time  $\varepsilon$  was replaced by a larger one, and thus the reaction zone was made much wider than the physical one. Recently, a modified fractional step method was introduced [15], where the structure of the Riemann solution of the homogeneous part was used to determine where burning should occur in each time step. This recipe works within the framework of the Godunov-type methods.

Recently, we proposed the random projection method as a general and systematic method to solve hyperbolic systems with stiff reaction term, applicable to reacting flow problems [1]. Unlike the random choice method of Chorin for reacting flow [7], which was originated from Glimm's scheme [12], and requires solving a generalized Riemann problem for hyperbolic systems with source terms [4], our method is a fractional step method, which combines a standard—no Riemann solver is needed—shock capturing method for the homogeneous convection with a strikingly simple random

projection step for the reaction terms. In the random projection step, the ignition temperature is chosen to be a uniformly distributed random variable between the two stable equilibria. At each time step, this random projection will move the shock by at most one grid point. The statistical average, however, yields the correct speed, even though the small time scale  $\varepsilon$  is not numerically resolved. In particular, when the random number is chosen to be the equidistributed van der Corput sampling sequence [14], [8] we have proven, for a model scalar problem, a first order accuracy on the shock speed if a monotonicity-preserving method, which includes all TVD schemes, is used in the convection step [1], [2]. A large amount of numerical experiments for one- and two-dimensional detonation waves demonstrate the robustness of this novel approach.

The generality of the random projection method lies in the fact that it applies to *any* shock capturing method for the homogeneous part, while other approaches, such as the ideas of [7], [15], are restricted to Godunov-type methods that require Riemann or generalized Riemann solvers.

In this paper, we conduct extensive numerical experiments to examine the applicability of the random projection method for reacting flows. We focus on stiff detonation waves and their interactions with other waves, including the interaction of detonation waves. Since the aim is to test the validity of an underresolved numerical method, which completely ignores the details of the reaction zone but captures all the main features of the solution outside the reaction zone, it is adequate to formulate this method using the reacting flow model of instantaneous reaction (with zone-width reaction zone, the so-called Chapman–Jouguet (C-J) model [10]), as given by [7], in which the chemical heat is released instantaneously:

$$(1.4) \quad U_t + F(U)_x + G(U)_y = 0,$$

$$(1.5) \quad U = \begin{pmatrix} \rho \\ m \\ n \\ e \end{pmatrix}, \quad F(U) = \begin{pmatrix} m \\ m^2/\rho + p \\ mn/\rho \\ m(e+p)/\rho \end{pmatrix}, \quad G(U) = \begin{pmatrix} n \\ mn/\rho \\ n^2/\rho + p \\ n(e+p)/\rho \end{pmatrix},$$

with equation of state

$$(1.6) \quad p = (\gamma - 1) \left( e - \frac{1}{2} (m^2 + n^2) / \rho - q_0 \rho z \right),$$

and the fraction of unburnt gas

$$(1.7) \quad z = \begin{cases} 0 & \text{if } T > T_c, \\ 1 & \text{if } T < T_c. \end{cases}$$

Formally, when the reaction time goes to zero, (1.1)–(1.3) with Arrhenius or Heaviside kinetics reduce effectively to this model. Although this “zero reaction limit” is not rigorously justified mathematically, the numerical comparisons between the random projection method based on this model with the resolved calculations based on the original kinetics of Arrhenius or Heaviside, as carried out later in this paper, do support the validity of this reduction unless one wants the full details of the reaction layer.

There certainly are restrictions with the instantaneous reaction model, or more generally, with any underresolved numerical method. First, if one needs the details of

the reaction layer, then one does need to numerically resolve the layer by solving the full equations (1.1)–(1.3) using fine meshes. Second, these methods cannot predict the instability in overdrive detonation waves, since, by ignoring the reaction layer, the peak value of pressure, which oscillates due to the instability, cannot be accurately computed. In order to obtain such fine structures, one has no choice but to use fine meshes, at least around the reaction zone by using techniques such as the adaptive mesh refinements.

The random projection method consists of two steps, the first being any standard shock capturing method for (1.4), followed by a random projection for the fraction variable  $z$  in (1.7), in which the ignition temperature  $T_c$  is replaced by a uniformly distributed random sequence. Here, the convection step is slightly simpler than the original one proposed in [1], where the full convection equation, including the homogeneous part of the species equation in (1.1)–(1.3), is solved. Algorithms for the collision of detonation waves are also introduced. Many numerical examples, including the C-J detonation, strong detonation, collisions of detonation with shocks, rarefaction wave, or another detonation, as well as two dimensional examples, will be used to justify the robustness of this novel approach.

The paper is organized as follows. In section 2 we provide a random projection method for the problem (1.4)–(1.7) in one space dimension with general initial data. Algorithms for multidetonations are also introduced. In section 3 this method is extended to two space dimension. In section 4 many numerical examples will be presented. In section 5 some conclusions are drawn.

**2. One-dimensional detonations.** In this section, we shall describe the random projection method for (1.4)–(1.7) in one space dimension. Moreover, we will describe its implementation for the case of interaction of detonation waves. The problem to be solved is given by

$$(2.1) \quad U_t + F(U)_x = 0,$$

$$(2.2) \quad U = \begin{pmatrix} \rho \\ m \\ e \end{pmatrix}, \quad F(U) = \begin{pmatrix} m \\ m^2/\rho + p \\ m(e + p)/\rho \end{pmatrix},$$

with equation of state

$$(2.3) \quad p = (\gamma - 1) \left( e - \frac{1}{2} m^2/\rho - q_0 \rho z \right),$$

and the fraction of unburnt gas

$$(2.4) \quad z = \begin{cases} 0 & \text{if } T > T_c, \\ 1 & \text{if } T < T_c. \end{cases}$$

Let the grid points be  $x_i$ ,  $i = \dots, -1, 0, 1, \dots$ , with equal mesh spacing  $h = x_{i+1} - x_i$ . The time level  $t_0 = 0$ ,  $t_1, t_2, \dots$  are also uniformly spaced with time step  $k = t_{n+1} - t_n$ . We use  $U_i^n = (\rho_i^n, m_i^n, e_i^n, (\rho z)_i^n)$  to denote the approximate solution of  $U = (\rho, m, e, \rho z)$  at the point  $(x_i, t_n) = (ih, nk)$ . Our main interest is an underresolved numerical method which allows  $k = O(h) \gg \varepsilon$  and still obtains physically relevant numerical solutions.

The random projection method is a fractional step method that consists of a standard shock capturing method for (2.1), denoted by  $S_F(k)$  for one time step,

followed by a random projection step for the fraction variable  $z$  defined by (2.4) where  $T_c$ , the ignition temperature, is randomized in a suitable domain. Let  $U^{n+1} = S_F(k)U^n$ . To obtain  $z^{n+1}$ , we replace (2.4) by

$$(2.5) \quad z_j^{n+1} = \begin{cases} 0 & \text{if } T_j^{n+1} > \theta_n, \\ 1 & \text{if } T_j^{n+1} < \theta_n, \end{cases}$$

where  $T_j^{n+1} = p_j^{n+1}/\rho_j^{n+1}$  and  $\theta_n$  is a random number, chosen one per time step, between two equilibrium temperatures on both sides of the detonation. To be more precise, consider the initial data

$$(2.6) \quad (\rho(x, 0), u(x, 0), p(x, 0), z(x, 0)) = \begin{cases} (\rho_l(x), u_l(x), p_l(x), 0) & \text{if } x \leq x_0, \\ (\rho_r(x), u_r(x), p_r(x), 1) & \text{if } x > x_0, \end{cases}$$

where  $x_0$  is a given point. Without loss of generality these data are chosen such that the detonation, initially at  $x = x_0$ , moves to the right. The case when the detonation moved to the left can be treated similarly. Since our projection always makes  $z$  either 1 or 0, therefore, at any time step  $t_n$ , there is an  $l(n) = j_0$ ,  $j_0$  an integer, such that

$$(2.7) \quad z_j^n = \begin{cases} 0 & \text{if } j \leq l(n), \\ 1 & \text{if } j > l(n). \end{cases}$$

Here  $l(n)$  is the location of the jump for  $z$  in the approximate solution at time  $t_n$  and we assume  $x_0 = l(0)h$  to be a grid point. Let

$$(2.8) \quad \theta_n = (T_l - T_r)\vartheta_n + T_r, \quad T_l = \min_{x < x_0} \frac{p_l(x, 0)}{\rho_l(x, 0)}, \quad T_r = \max_{x > x_0} \frac{p_r(x, 0)}{\rho_r(x, 0)}$$

with  $\vartheta_n$  being the van der Corput sampling sequence on the interval  $[0, 1]$ .

The van der Corput sequence is an equidistributed sequence with the minimal deviation among all random sequences [14]. It is obtained as follows: let  $1 \leq n = \sum_{k=0}^m i_k 2^k$ ,  $i_k = 0, 1$ , be the binary expansion of the integer  $n$ . One gets  $\vartheta_n$  on  $[0, 1]$  as

$$(2.9) \quad \vartheta_n = \sum_{k=0}^m i_k 2^{-(k+1)}, \quad n = 1, 2, \dots$$

Since there are other waves in the domain, one cannot project  $z$  according to (2.5) in the whole domain. Instead, we do it around the denotation, a procedure called the *local random projection* in [1]. Specifically, we move the jump of  $z$  according to the following algorithm:

$$(2.10) \quad \begin{aligned} S_{sp}(k) : \quad & \text{set } l(n+1) := l(n) - 1; \\ & \text{For } l = l(n) - 1, l(n), \dots, l(n) + d, \text{ do} \\ & \quad l(n+1) := l \quad \text{if } T_l^{n+1} > \theta_n; \\ & \quad z_j^{n+1} = \begin{cases} 0 & \text{if } j \leq l(n+1) \\ 1 & \text{if } j > l(n+1) \end{cases} \quad \text{for all } j, \end{aligned}$$

where  $d$  is the number of smeared points in the shock layer. In the above algorithm, only  $d + 2$  points will be scanned.

The stability condition for this algorithm, as well as the algorithms for multidetonations (2.15) and (2.20), is the usual CFL condition determined by the operator  $S_F(k)$  for the convection terms.

In our numerical comparison, we will compare the random projection method with the *deterministic* projection method which projects the fraction of unburnt gas,  $z$ , after the convection step according to the *fixed* ignition temperature  $T_c$  in (2.4).

We now extend the random projection method to handle the problems involving more than one detonation wave. For clarity of presentation we present only the case of two detonations. It is straightforward to extend to the case where there are more than two detonations.

Consider (2.1)–(2.4) with initial data

$$(2.11) \quad (\rho(x, 0), u(x, 0), p(x, 0), z(x, 0)) = \begin{cases} (\rho_l(x), u_l(x), p_l(x), 0) & \text{if } x \leq x_1, \\ (\rho_m(x), u_m(x), p_m(x), 1) & \text{if } x_1 < x < x_2, \\ (\rho_r(x), u_r(x), p_r(x), 0) & \text{if } x_2 \leq x. \end{cases}$$

These data are chosen such that the two detonations move toward each other; i.e., the detonation initially at  $x = x_1$  moves to the right and the one initially at  $x = x_2$  moves to the left. Thus after some time, the two detonations will collide.

Let

$$(2.12) \quad T_l = \min_{x < x_1} \frac{p_l(x)}{\rho_l(x)}, \quad T_m = \max_{x_1 < x < x_2} \frac{p_m(x)}{\rho_m(x)}, \quad T_r = \min_{x > x_2} \frac{p_r(x)}{\rho_r(x)}$$

and

$$(2.13) \quad \theta_n^{(1)} = (T_l - T_m)\vartheta_n + T_m, \quad \theta_n^{(2)} = (T_r - T_m)\vartheta_n + T_m.$$

Since the projection always makes  $z$  either 1 or 0, the profile of  $z$  at any time step is a piecewise constant function. Therefore, at any time step  $t_n$ , there are  $l_1(n) = j_1$  and  $l_2(n) = j_2$  with  $j_1 \leq j_2$  integers such that

$$(2.14) \quad z_j^n = \begin{cases} 0 & \text{if } j \leq l_1(n), \\ 1 & \text{if } l_1(n) < j < l_2(n), \\ 0 & \text{if } l_2(n) \leq j. \end{cases}$$

Here we assume that  $x_1 = l_1(0)h$  and  $x_2 = l_2(0)h$  are grid points. Since  $x_1 \leq x_2$ , then  $l_1(0) \leq l_2(0)$ . One can use the following algorithm to obtain  $z^{n+1}$  if the positions of the two detonations at time  $t_n$ , i.e.,  $l_1(n)$  and  $l_2(n)$ , are known. The detailed algorithm to find  $z^{n+1}$  is as follows:

$$(2.15) \quad \begin{aligned} S_{cp}(k) : \quad & l_{\text{mid}} = (l_1(n) + l_2(n))/2; \\ & \text{set } l_1(n+1) := l_1(n) - 1; \\ & \text{For } l = l_1(n) - 1, l_1(n), \dots, \min\{l_1(n) + d, l_{\text{mid}} + 1\} \text{ do} \\ & \quad l_1(n+1) := l \quad \text{if } T_l^{n+1} > \theta_n^{(1)}; \\ & \text{set } l_2(n+1) := l_2(n) + 1; \\ & \text{For } l = l_2(n) + 1, l_2(n), \dots, \max\{l_2(n) - d, l_{\text{mid}} - 1\} \text{ do} \\ & \quad l_2(n+1) := l \quad \text{if } T_l^{n+1} > \theta_n^{(2)}; \\ & z_j^{n+1} = \begin{cases} 0 & \text{if } j \leq l_1(n+1) \\ 1 & \text{if } l_1(n+1) < j < l_2(n+1) \\ 0 & \text{if } l_2(n+1) \leq j \end{cases} \quad \text{for all } j. \end{aligned}$$

This algorithm still works even after the detonations have collided and then become extinct. After the detonations have collided, the fraction of unburnt gas  $z \equiv 0$ . From this algorithm, once  $l_1(n) \geq l_2(n)$  at some time step  $t = t_n$ , then  $l_1(n + 1) \geq l_2(n + 1)$  for the next step. Thus the profile of  $z^{n+1}$  determined from (2.15) is the zero function.

Another case is when two detonations move away from each other. Consider the initial data

$$(2.16) \quad (\rho(x, 0), u(x, 0), p(x, 0), z(x, 0)) = \begin{cases} (\rho_l(x), u_l(x), p_l(x), 1) & \text{if } x < x_1, \\ (\rho_m(x), u_m(x), p_m(x), 0) & \text{if } x_1 \leq x \leq x_2, \\ (\rho_r(x), u_r(x), p_r(x), 1) & \text{if } x_2 < x. \end{cases}$$

These data are chosen such that the two detonations move away from each other; i.e., the detonation initially at  $x = x_1$  moves to the left and the one initially at  $x = x_2$  moves to the right. In this case, there is no collision of detonations at all.

Let

$$(2.17) \quad T_l = \max_{x < x_1} \frac{p_l(x)}{\rho_l(x)}, \quad T_m = \min_{x_1 < x < x_2} \frac{p_m(x)}{\rho_m(x)}, \quad T_r = \max_{x > x_2} \frac{p_r(x)}{\rho_r(x)}$$

and

$$(2.18) \quad \theta_n^{(1)} = (T_m - T_l)\vartheta_n + T_l, \quad \theta_n^{(2)} = (T_m - T_r)\vartheta_n + T_r.$$

At any time step  $t_n$ , there are  $l_1(n) = j_1$  and  $l_2(n) = j_2$  with  $j_1 \leq j_2$  integers such that

$$(2.19) \quad z_j^n = \begin{cases} 1 & \text{if } j < l_1(n), \\ 0 & \text{if } l_1(n) \leq j \leq l_2(n), \\ 1 & \text{if } l_2(n) < j. \end{cases}$$

The detailed algorithm to find  $z^{n+1}$  is as follows:

$$(2.20) \quad \begin{aligned} S_{bp}(k) : & \text{ set } l_1(n + 1) := l_1(n) + 1; \\ & \text{ For } l = l_1(n) + 1, l_1(n), \dots, l_1(n) - d, \text{ do} \\ & \quad l_1(n + 1) := l \quad \text{if } T_l^{n+1} > \theta_n^{(1)}; \\ & \text{ set } l_2(n + 1) := l_2(n) - 1; \\ & \text{ For } l = l_2(n) - 1, l_2(n), \dots, l_2(n) + d, \text{ do} \\ & \quad l_2(n + 1) := l \quad \text{if } T_l^{n+1} > \theta_n^{(2)}; \\ z_j^{n+1} = & \begin{cases} 1 & \text{if } j < l_1(n + 1) \\ 0 & \text{if } l_1(n + 1) \leq j \leq l_2(n + 1) \\ 1 & \text{if } l_2(n + 1) < j \end{cases} \quad \text{for all } j. \end{aligned}$$

*Remark 2.1.* The algorithms presented in this section rely on the assumption that initially the detonation front is already formed. Thus it cannot be used to predict the creation of a detonation from a completely unburnt gas (when the initial value of  $z$  is identically zero in the entire domain). Since the detonation will be formed beyond the initial layer, one can use a refined calculation within the initial layer and then use the random projection method beyond the initial layer. While one can afford to resolve the initial layer with a refined computation, it is certainly more advantageous to use an underresolved numerical method for all later time beyond the initial layer.

**3. The two-dimensional method.** In this section, the random projection method is extended to the two space dimensional problem (1.4)–(1.7). For simplicity, we consider the detonation waves in a two-dimensional channel. Let the initial data be

$$(3.1) \quad (\rho(x, y, 0), u(x, y, 0), v(x, y, 0), p(x, y, 0), z(x, y, 0)) = \begin{cases} (\rho_l, u_l, 0, p_l, 0) & \text{if } x \leq \xi(y), \\ (\rho_r, u_r, 0, p_r, 1) & \text{if } x > \xi(y), \end{cases}$$

where  $\xi(y)$  is a given function of  $y$  and these data are chosen such that the detonation moves to the right. Let

$$(3.2) \quad \theta_n = (T_l - T_r)\vartheta_n + T_r, \quad T_l = \frac{p_l}{\rho_l}, \quad T_r = \frac{p_r}{\rho_r}$$

with  $\vartheta_n$  (see (2.9) for detail) being the van der Corput sampling sequence on the interval  $[0, 1]$ .

Let the grid points  $(x_i, y_j) = (ih, jh)$ ,  $i, j = \dots, -1, 0, 1, \dots$ , with equal mesh spacing  $h$ . The time level  $t_n = nk$ ,  $k = 0, 1, 2, \dots$ , are also uniformly spaced with time step  $k$ . Let  $U_{i,j}^n = (\rho_{i,j}^n, m_{i,j}^n, n_{i,j}^n, e_{i,j}^n, (\rho z)_{i,j}^n)$  be the approximate solution of  $U = (\rho, m, n, e, (\rho z))$  at  $(x_i, y_j, t_n) = (ih, jh, nk)$ . Let  $S_{FG}(k)$  be a standard shock capturing method for (1.4). Notice that, at any time step, for each  $j$ , there is an  $l_j(n) = j_n$ ,  $j_n$  an integer such that

$$(3.3) \quad z_{i,j}^n = \begin{cases} 0 & \text{if } j \leq l_j(n), \\ 1 & \text{if } i > l_j(n). \end{cases}$$

Here,  $l_j(n)$  is the location of the jump for  $z$  at the grid line  $y = y_j$  in the approximate solution at time  $t_n = nk$ . Then the random project algorithm to find  $z^{n+1}$  is as follows:

$$(3.4) \quad \begin{aligned} S_{2p}(k) : & \text{ For } j \text{ do} \\ & \text{ Set } l_j(n+1) := l_j(n) - 1, \\ & \text{ For } l = l_j(n) - 1, l_j(n), \dots, l_j(n) + d, \text{ do} \\ & \quad l_j(n+1) := l \quad \text{if } T_{l,j}^{n+1} > \theta_n; \\ & z_{i,j}^{n+1} = \begin{cases} 0 & \text{if } i \leq l_j(n+1) \\ 1 & \text{if } i > l_j(n+1) \end{cases} \quad \text{for all } i. \end{aligned}$$

The stability condition for this algorithm is still the usual CFL condition determined from the convection step  $S_{FG}(k)$ .

Although the above algorithm is written for a detonation traveling in the direction of the  $x$ -axis, little additional effort is needed to extend it to more general cases where the detonation front moves toward all possible directions. One such example is given in the next section (Example 4.8) where the detonation is advancing in circular direction.

**4. Numerical examples.** In order to verify the performance of the random projection method proposed in this paper, we conduct extensive numerical experiments, including the C-J detonation, strong detonation, collision of a detonation with a shock, a rarefaction wave, and another detonation. We also give two-dimensional examples. In our computation, the operators  $S_F(k)$  and  $S_{FG}(k)$  are chosen as the second order relaxed scheme [17], which is a TVD scheme without the usage of Riemann solvers or local characteristic decompositions. We choose  $d = 5$  in (2.10), (2.15), (2.20), and (3.4) in our computations in this section.



In this section, we compare our numerical results with the resolved solutions. The resolved ones are obtained by solving (1.1)–(1.3) with Heaviside kinetics with a fractional step approach that consists of a second order relaxed scheme for the homogeneous part in (1.1) for one time step, followed by an implicit backward Euler scheme for the chemical reaction. One can see the details in [1] and [11]. Resolved computations based on the Arrhenius kinetics vary only the detailed structure of the reaction zones, so it will not be reported here since the goal of the paper is not to get the accurate reaction zone but all the macroscopic structures outside the reaction zone.

*Example 4.1* (C-J detonation). This is Example 4.1 in [1] revisited. We choose here the case of ozone decomposition C-J detonation discussed and computed in [9] and [4]. We use CGS units and the following parameter values:

$$\gamma = 1.4, \quad q_0 = 0.5196 \times 10^{10}, \quad \frac{1}{\varepsilon} = K = 0.5825 \times 10^{10}, \quad T_c = 0.1155 \times 10^{10}.$$

The initial data are taken as the piecewise constant data defining a C-J detonation as a single wave. (Recall that in the C-J model a C-J detonation corresponds to a sonic detonation, or, in other words, a sharp reaction wave that moves at minimal speed relative to the unburnt gas.) The reaction rate  $K$  in all the examples is irrelevant for the projection method but is needed for the resolved calculations. The initial state was given by

$$(\rho, u, p, z)(x, 0) = \begin{cases} (\rho_l, u_l, p_l, 0) & \text{if } x \leq 0.005, \\ (\rho_r, u_r, p_r, 1) & \text{if } x > 0.005, \end{cases}$$

where  $p_l = p_{C,J} = 6.270 \times 10^6$ ,  $\rho_l = \rho_{C,J} = 1.945 \times 10^{-3}$ ,  $u_l = u_{C,J} = 4.162 \times 10^4$ ; and  $p_r = 8.321 \times 10^5$ ,  $\rho_r = 1.201 \times 10^{-3}$ ,  $u_r = 0$ . The speed of the sharp front in this example is  $D = D_{C,J} = 1.088 \times 10^5$ . In this example, the width of the reaction zone is approximately  $5 \times 10^{-5}$  [4], [9]. This width is irrelevant for the underresolved calculation but is used for the resolved calculation and for a comparison with the mesh size to check whether the calculation is resolved or underresolved.

This problem is solved on the interval  $[0, 0.05]$ . The “exact” solution is obtained by using a resolved calculation with  $h = 5 \times 10^{-6}$  (i.e., 10001 grid points on the interval  $[0, 0.05]$ ) and  $k = 5 \times 10^{-12}$ . The mesh size and time step resolve the chemical scale. Now we compare the results obtained by the random projection method and the deterministic method when the reaction scale is underresolved. We use  $h = 5 \times 10^{-4}$  (i.e., 101 grid points for the interval  $[0, 0.05]$ ) and  $k = 5 \times 10^{-10}$  and output the numerical solution at  $t = 2 \times 10^{-7}$ .

Figure 4.1(a) shows the numerical solution by using the random projection method (2.10), while Figure 4.1(b) shows the numerical solution obtained by the deterministic method. It can be seen that the random projection method can capture the correct speed of the discontinuity of the C-J detonation wave even when the chemical reaction scale is not numerically resolved. As mentioned earlier, with an underresolved method it is impossible to capture the pressure spike which has a width in the order of reaction scale  $\varepsilon$ . There are small postshock statistical fluctuations due to the random nature of the method, but they are at an acceptable level. The deterministic method produces spurious waves, as was observed in earlier literatures.

In all of the following examples, the deterministic method always produces spurious waves when the chemical scale is not resolved. We will not report those results and will present only the solutions obtained by the random projection method.

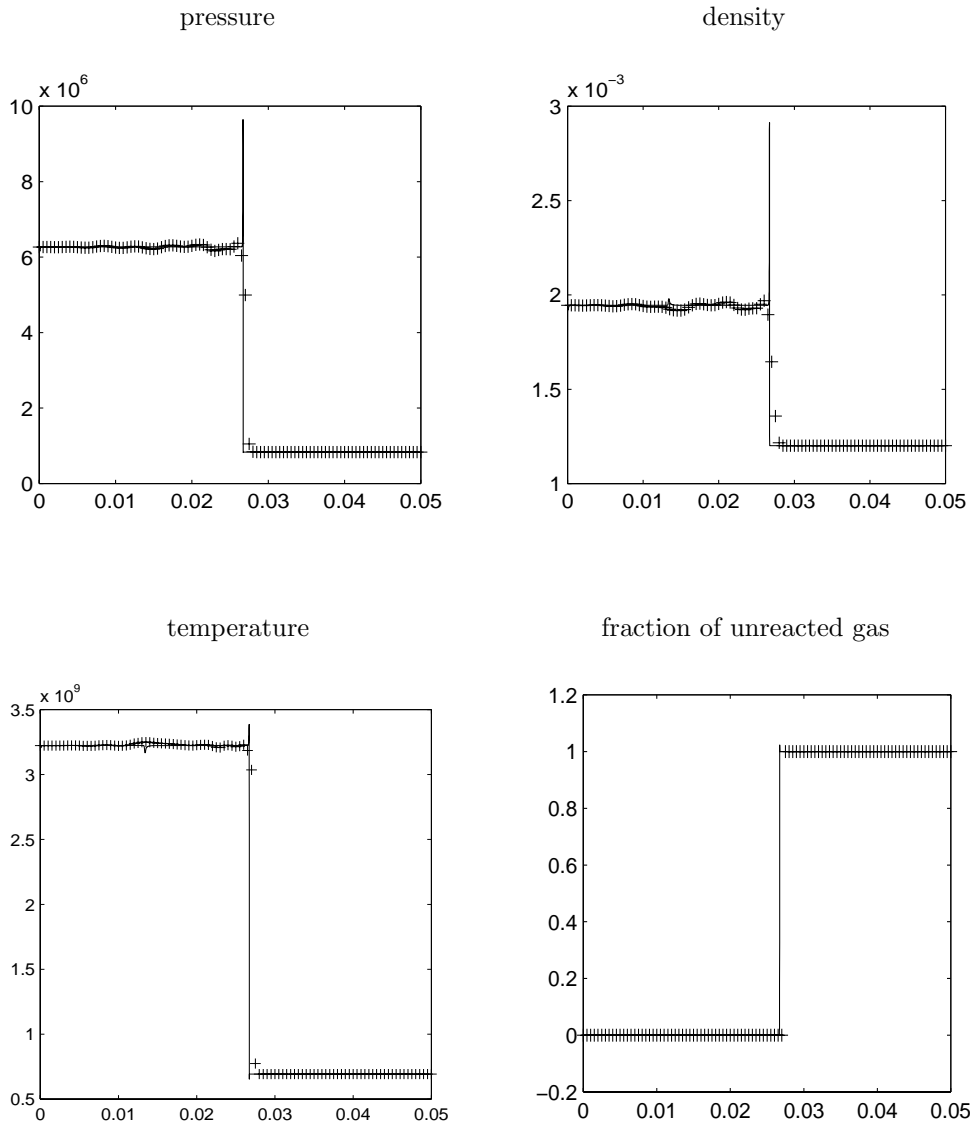


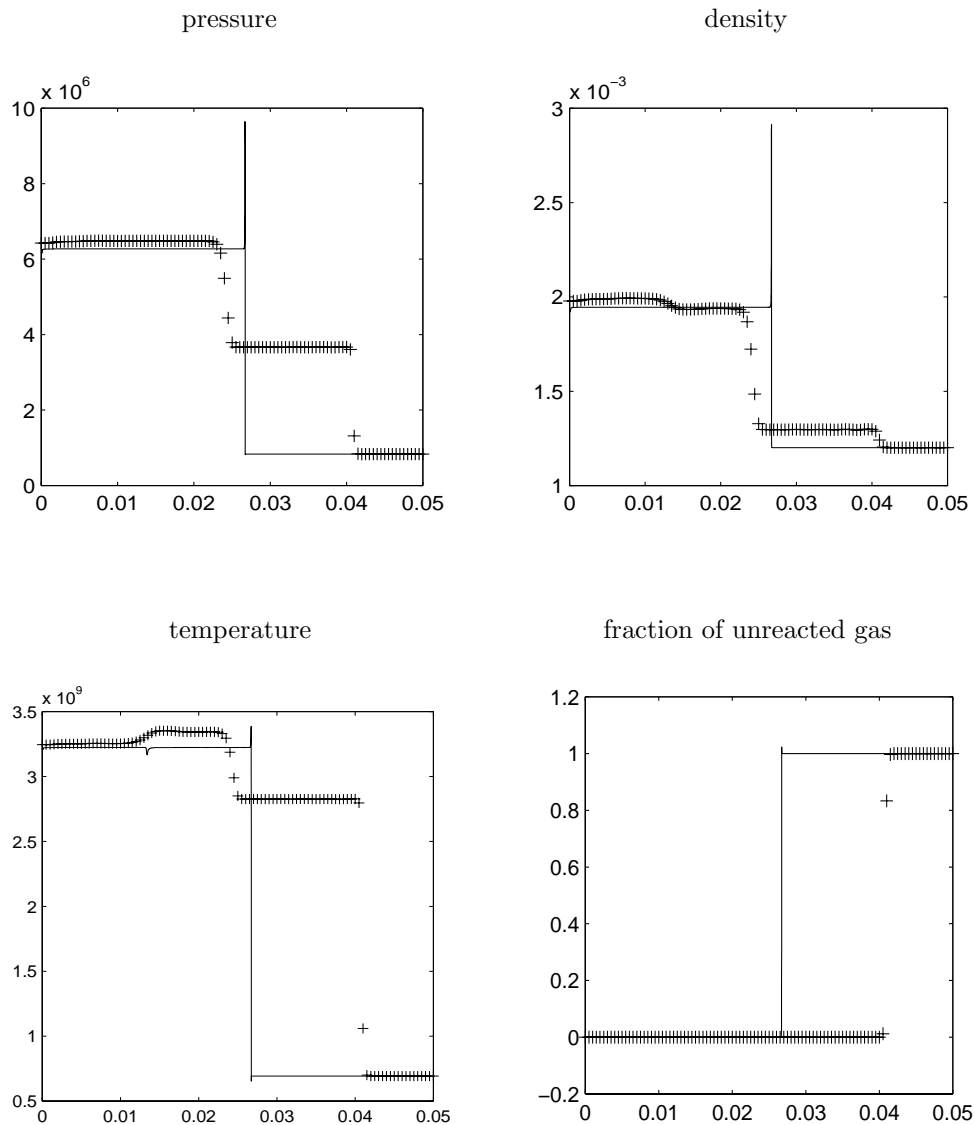
FIG. 4.1. Numerical solutions of Example 4.1 at  $t = 2 \times 10^{-7}$  calculated with  $h = 5 \times 10^{-4}$ ,  $k = 5 \times 10^{-10}$ . -: “exact” solutions; ++: computed solutions. (a) The random projection method.

Example 4.2 (a strong detonation). This is Example 4.3 in [1] revisited. The setup of this example is similar to those in Example 4.1 (i.e.,  $\gamma$ ,  $q_0$ ,  $K = \frac{1}{\varepsilon}$ , and  $T_c$  are the same), except that the initial data are changed to

$$(\rho, u, p, z)(x, 0) = \begin{cases} (\rho_l, u_l, p_l, 0) & \text{if } x \leq 0.005, \\ (\rho_r, u_r, p_r, 1) & \text{if } x > 0.005, \end{cases}$$

where  $u_l = 9.162 \times 10^4 > u_{CJ}$ ,  $\rho_l = \rho_{CJ}$ ,  $p_l = 8.27 \times 10^6 > p_{CJ}$ , and  $p_r, u_r, \rho_r, p_{CJ}, u_{CJ}$ , and  $\rho_{CJ}$  are the same as those in Example 4.1. In this case there is a strong detonation, a contact discontinuity, and a shock, all moving to the right.

The “exact” solution is obtained similarly as that in Example 4.1. Figure 4.2

FIG. 4.1 (cont.). (b) *The deterministic method.*

shows the numerical solutions by the random projection method (2.10) with  $h = 5 \times 10^{-4}$  (i.e., 101 grid points for the interval  $[0, 0.05]$ ) and  $k = 5 \times 10^{-10}$  at time  $t = 2 \times 10^{-7}$ .

*Example 4.3* (collision of a detonation with a rarefaction wave). We choose  $\gamma = 1.2$ ,  $q_0 = 50$ ,  $T_c = 3.0$ , and  $\frac{1}{\varepsilon} = K = 230.75$ . The data are taken from [16]. The initial state was given by

$$(\rho, u, p, z)(x, 0) = \begin{cases} (\rho_l, u_l, p_l, 0) & \text{if } x \leq 10, \\ (\rho_m, u_m, p_m, 0) & \text{if } 10 < x \leq 20, \\ (\rho_r, u_r, p_r, 1) & \text{if } 20 < x, \end{cases}$$

where  $p_l = 40.0$ ,  $\rho_l = 2.0$ ,  $u_l = 4.0$ ;  $p_m = 54.8244$ ,  $\rho_m = 3.64282$ ;  $u_m = 6.2489$ ; and

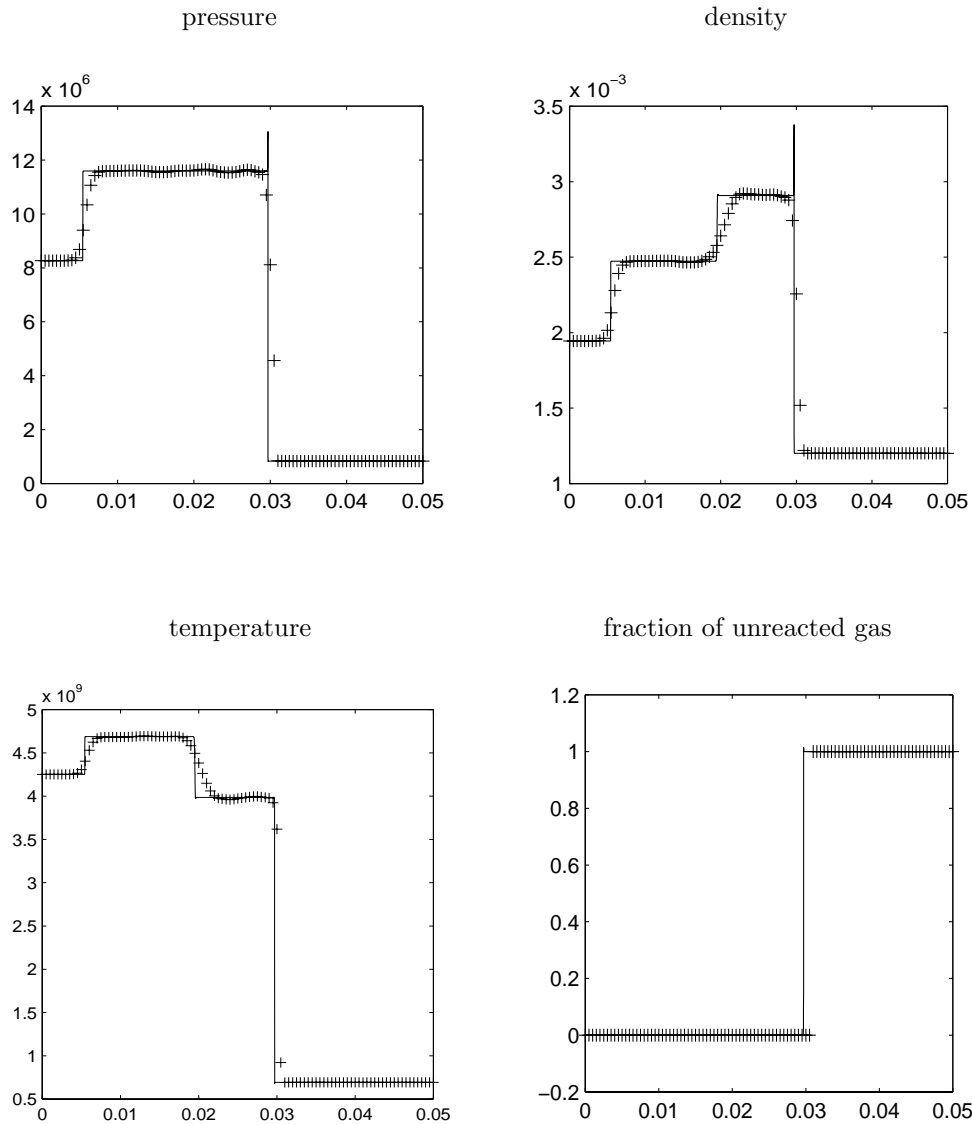


FIG. 4.2. Numerical results at  $t = 2 \times 10^{-7}$  for a strong detonation in Example 4.2 calculated by the random projection method (2.10).  $h = 5 \times 10^{-4}$ ,  $k = 5 \times 10^{-10}$ . -: “exact” solutions; ++: computed solutions.

$p_r = 1.0$ ,  $\rho_r = 1.0$ ,  $u_r = 0$ . By selecting these data, the “half reaction length”  $L_{\frac{1}{2}}$  is the spatial unit 1 [16]. This number is used to compare the mesh sizes in resolved and underresolved numerical experiments.

In this example, there is a right moving detonation, a right moving rarefaction wave, a right moving contact discontinuity, and a left moving rarefaction wave before the right moving rarefaction catches the detonation wave.

This problem is solved on the interval  $[0, 100]$ . The “exact” solution is obtained by using a resolved calculation  $h = 0.005$  (i.e., 20001 grid points on the interval  $[0, 100]$ ) and  $k = 0.00025$ .

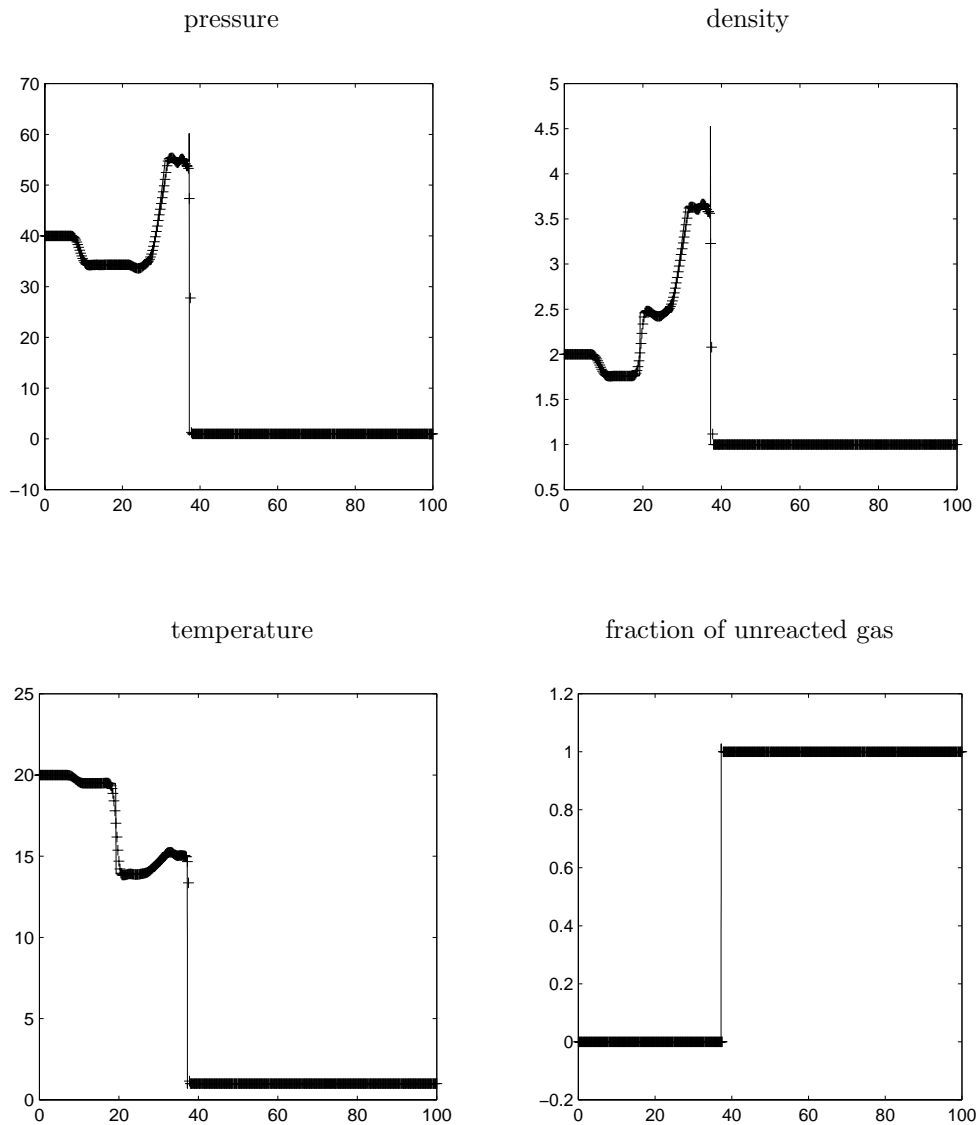


FIG. 4.3. Numerical results of Example 4.3 involving the collision of a detonation with a rarefaction wave using the random projection method (2.10).  $h = 0.25$ ,  $k = 0.01$ . —: “exact” solutions; ++: computed solutions. (a)  $t = 2$  (before collision).

Figure 4.3 shows the numerical solution by using the random projection method (2.10) with  $h = 0.25$  (i.e., 401 grid points for the interval  $[0, 100]$ ) and  $k = 0.01$  at time  $t = 2$  (before collision) and  $t = 8.0$  (after collision), respectively. After the collision, there are some small downstream wiggles which are numerical artifacts and do not appear in the resolved calculation.

*Example 4.4* (a detonation interacting with an oscillatory profile). The setup of this problem is similar to those in Example 4.3 (i.e.,  $\gamma$ ,  $q_0$ , and  $T_c$  are the same),

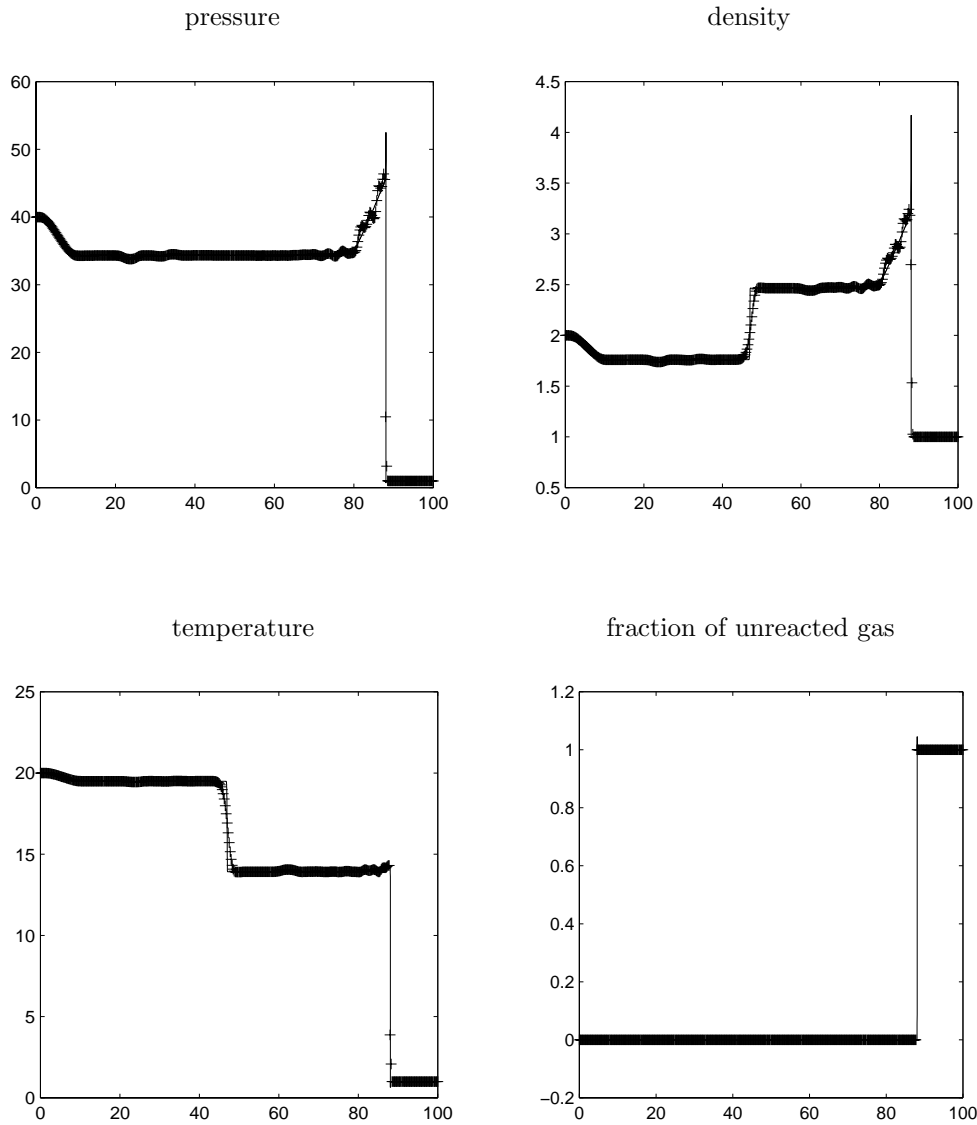


FIG. 4.3 (cont.). (b)  $t = 8$  (after collision).

except that we change  $K = 1000.0$  and the initial data to

$$(\rho, u, p, z)(x, 0) = \begin{cases} (\rho_l, u_l, p_l, 0) & \text{if } x \leq \frac{\pi}{2}, \\ (\rho_r(x), u_r, p_r, 1) & \text{if } \frac{\pi}{2} < x, \end{cases}$$

where  $p_l = 21.53134$ ,  $\rho_l = 1.79463$ ,  $u_l = 3.0151$ ; and  $p_r = 1.0$ ,  $\rho_r(x) = 1.0 + 0.5 \sin 2x$ ,  $u_r = 0$ .

This problem is solved on the interval  $[0, 2\pi]$ . The “exact” solutions are obtained by using  $h = \frac{\pi}{10000}$  (i.e., 20001 grid points on the interval  $[0, 2\pi]$ ) and  $k = \frac{h}{20}$ . This is a resolved calculation.

Figure 4.4 shows the numerical solutions by using the random projection method (2.10) with  $h = \frac{\pi}{400}$  (i.e., 801 grid points for the interval  $[0, 2\pi]$ ) and  $k = \frac{h}{20}$  at time

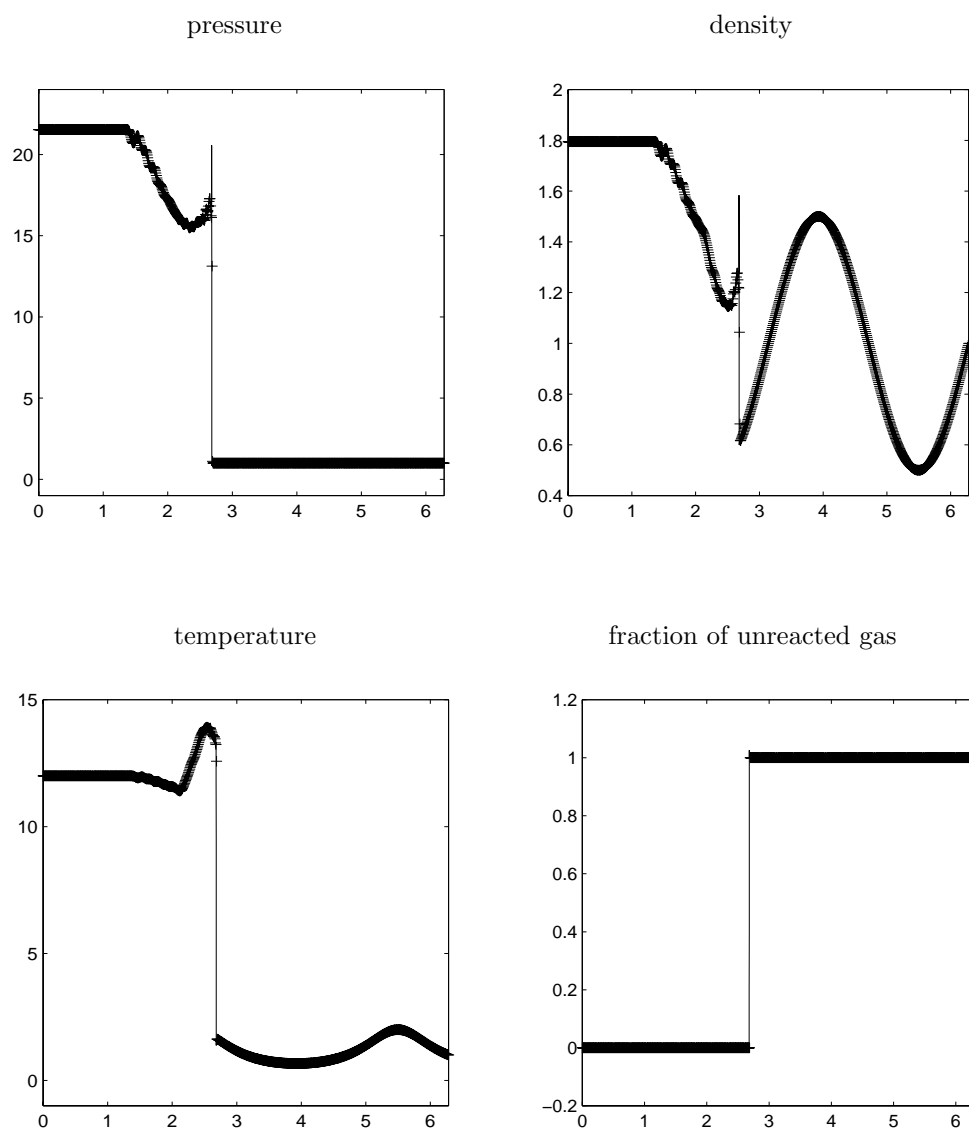


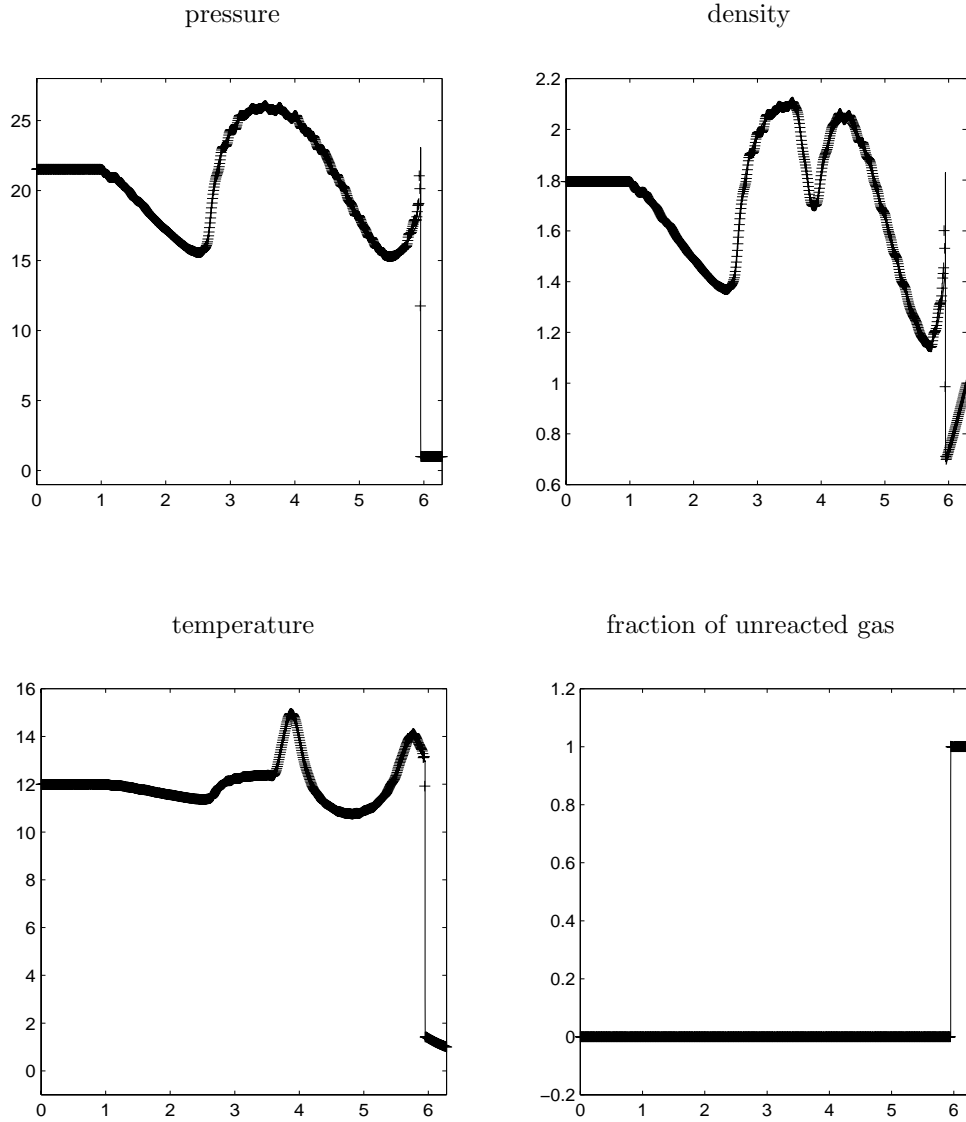
FIG. 4.4. Numerical results of Example 4.4 by the random projection method (2.10).  $h = \frac{\pi}{400}$ ,  $k = \frac{h}{20}$ . -: “exact” solutions; ++: computed solutions. (a)  $t = \frac{\pi}{20}$ .

$t = \frac{\pi}{20}$  and  $t = \frac{\pi}{5}$ , respectively.

*Example 4.5* (collision of a detonation with a shock, a contact discontinuity, and a rarefaction). The setup of this problem is similar to those in Example 4.3 (i.e.,  $\gamma$ ,  $q_0$ ,  $K = \frac{1}{\varepsilon}$ , and  $T_c$  are the same), except that we change the initial data to

$$(\rho, u, p, z)(x, 0) = \begin{cases} (\rho_l, u_l, p_l, 0) & \text{if } x \leq 10, \\ (\rho_m, u_m, p_m, 1) & \text{if } 10 < x \leq 40, \\ (\rho_r, u_r, p_r, 1) & \text{if } 40 < x, \end{cases}$$

where  $p_l = 54.8244$ ,  $\rho_l = 3.64282$ ,  $u_l = 6.2489$ ;  $p_m = 1.0$ ,  $\rho_m = 1.0$ ,  $u_m = 0.0$ ; and  $p_r = 10.0$ ,  $\rho_r = 4.0$ ,  $u_r = 0$ .

FIG. 4.4 (cont.). (b)  $t = \frac{\pi}{5}$ .

In this example, there is a right moving detonation, a right moving rarefaction, a stationary contact discontinuity, and a left moving shock before a series of collisions occur after the detonation catches up with the other waves.

The “exact” solution is obtained similarly as that in Example 4.3. Figures 4.5(a)–(c) show the numerical solution by using the random projection method (2.10) with  $h = 0.125$  (i.e., 801 grid points for the interval  $[0, 100]$ ) and  $k = 0.005$  at time  $t = 2$  (before collision)  $t = 4$  (between the collisions with the shock and with the rarefaction), and  $t = 8.0$  (after all collisions), respectively.

This example shows that the random projection method is able to handle the interactions between the detonation and all other waves of a compressible gas.

*Example 4.6* (collision of two detonations). The setup in this example is similar



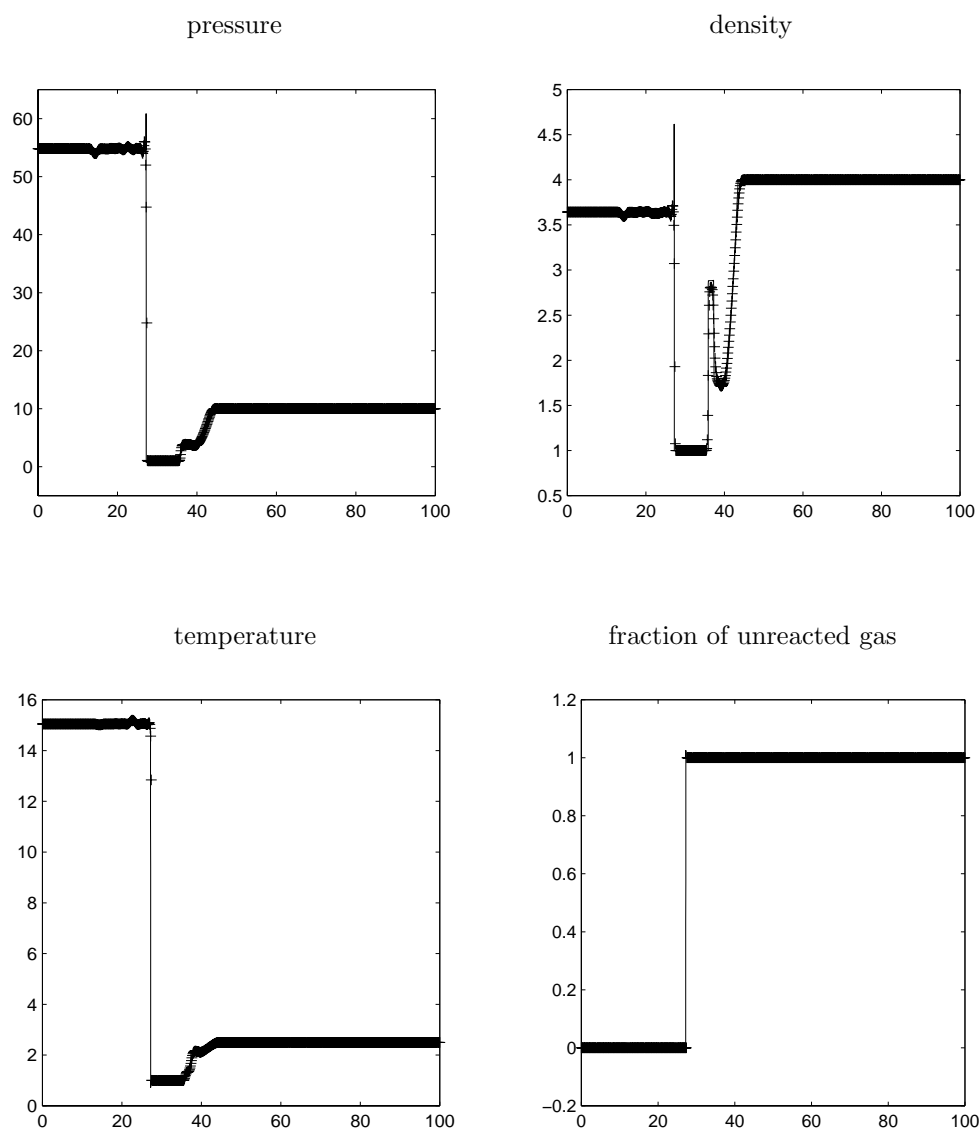


FIG. 4.5. Numerical results of Example 4.5 involving the collisions of a detonation with a shock and then a rarefaction wave by the random projection method (2.10).  $h = 0.125$ ,  $k = 0.005$ . -: “exact” solutions; ++: computed solutions. (a)  $t = 2$  (before collision).

to those in Example 4.3 (i.e.,  $\gamma$ ,  $q_0$ ,  $K = \frac{1}{\varepsilon}$ , and  $T_c$  are the same), except that we change the initial data to

$$(\rho, u, p, z)(x, 0) = \begin{cases} (\rho_l, u_l, p_l, 0) & \text{if } x \leq 10, \\ (\rho_m, u_m, p_m, 1) & \text{if } 10 < x < 90, \\ (\rho_r, u_r, p_r, 0) & \text{if } 90 \leq x, \end{cases}$$

where  $p_l = 30.0$ ,  $\rho_l = 1.79463$ ,  $u_l = 3.0151$ ;  $p_m = 1.0$ ,  $\rho_m = 1.0$ ,  $u_m = 0.0$ ; and  $p_r = 21.53134$ ,  $\rho_r = 1.79463$ ,  $u_r = -8.0$ .

In this example, there is a right moving detonation, a left moving strong det-

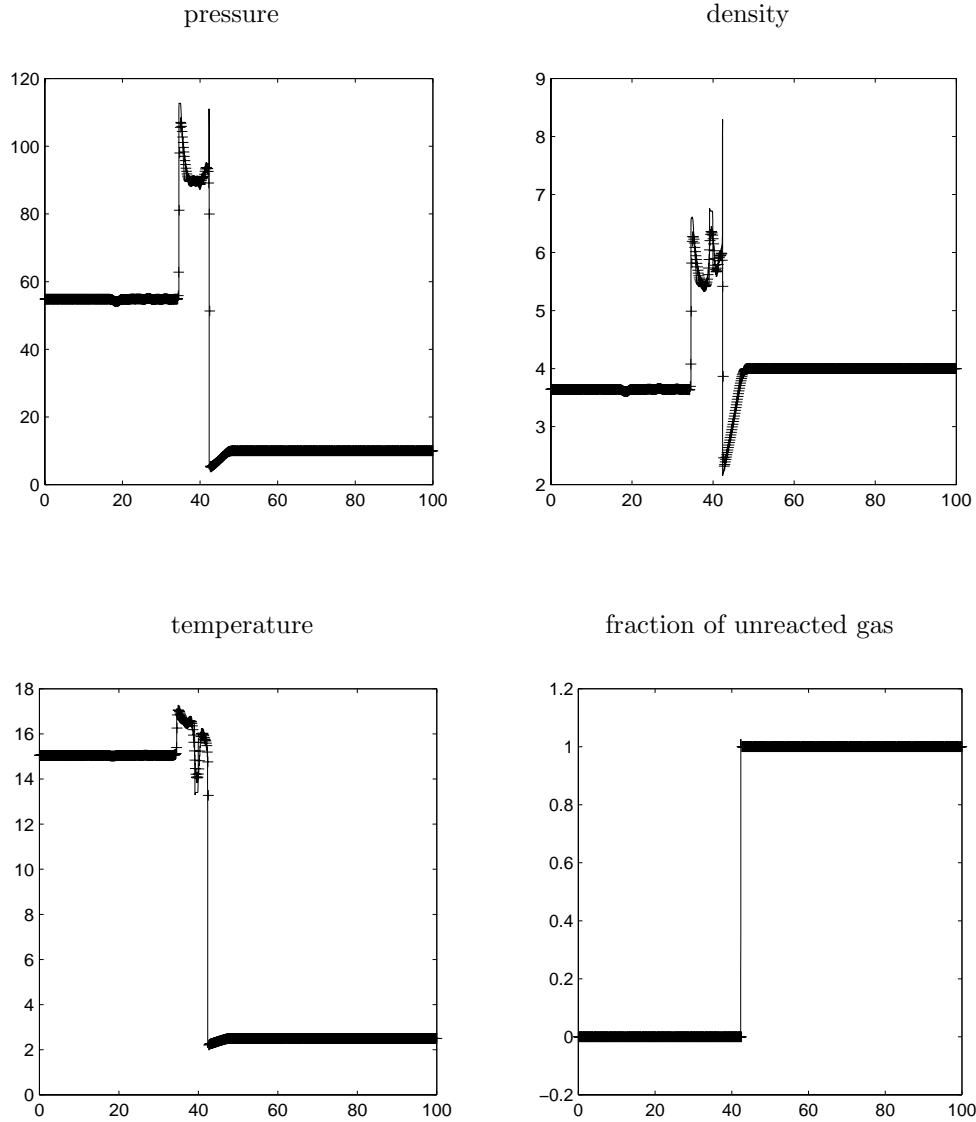


FIG. 4.5 (cont.). (b)  $t = 4$  (between the collisions with the shock and the rarefaction).

onation, and other waves. After some time, there is a collision between the two detonations.

The “exact” solution is obtained similarly as that in Example 4.3. Figure 4.6 shows the numerical solution by using the random projection method (2.15) with  $h = 0.25$  (i.e., 401 grid points for the interval  $[0, 100]$ ) and  $k = 0.01$  at time  $t = 4$  (before collision) and  $t = 6.0$  (after collision), respectively. After the collisions, the detonation becomes extinct and two shocks are formed. This example shows that the random projection is valid even after the detonation disappears.

From the above examples, we can see that the random projection method works very well for one-dimensional detonation wave problems even if the reaction scale is not numerically resolved. It not only captures the correct speeds of detonations but

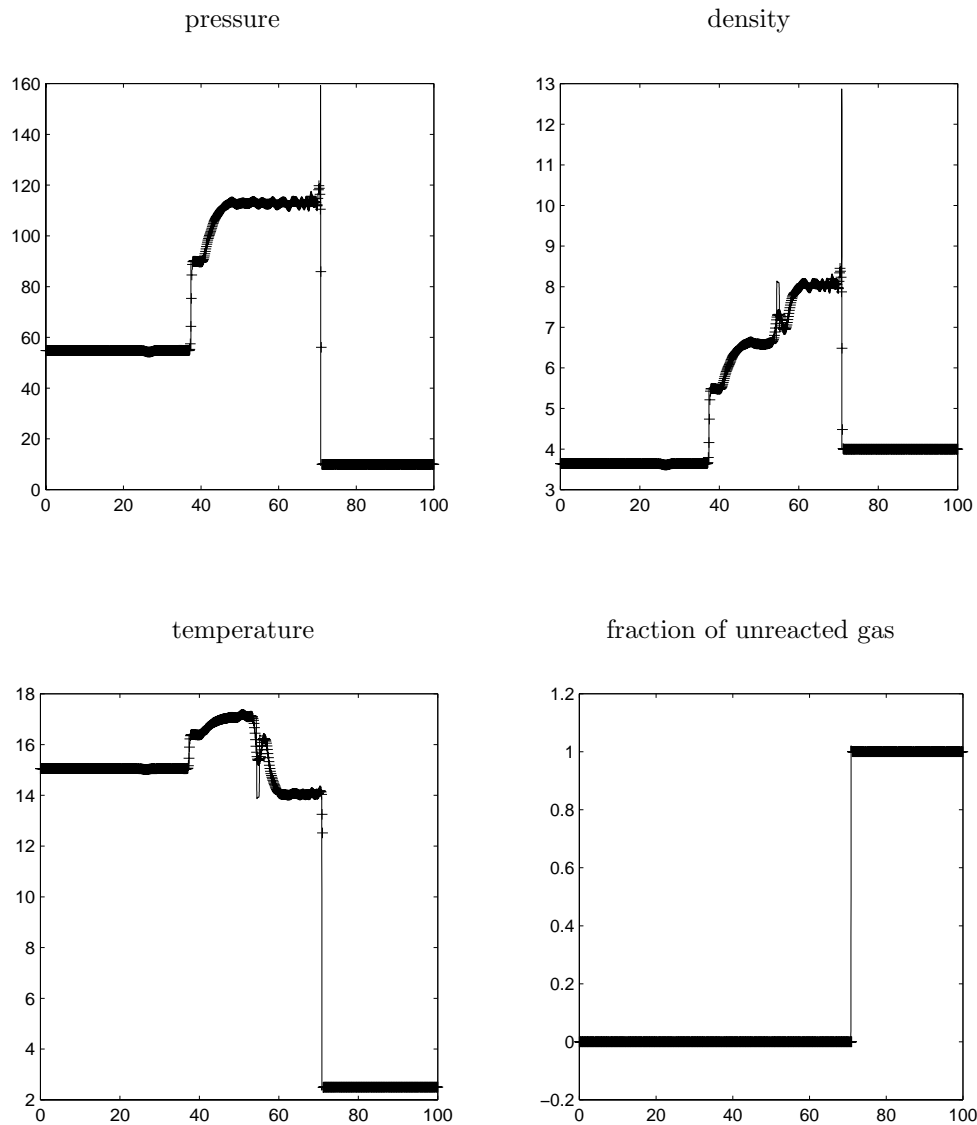


FIG. 4.5 (cont.). (c)  $t = 8$  (after all collisions).

also is able to handle the interactions between detonations and between a detonation with other waves of a compressible gas. Its applicability remains after the extinction of the detonation.

*Example 4.7* (a two-dimensional circular detonation front). We consider the problem (1.4)–(1.7) in a two-dimensional channel; the upper and lower boundaries are solid walls. We choose  $\gamma$ ,  $q_0$ ,  $K = \frac{1}{\varepsilon}$ , and  $T_c$  the same as those in Example 4.3. The initial data (3.1) are chosen as  $p_l = 54.8244$ ,  $\rho_l = 3.64282$ ,  $u_l = 6.2489$ ,  $v_l = 0.0$ ; and  $p_r = 1.0$ ,  $\rho_r = 1.0$ ,  $u_r = 0.0$ ,  $v_r = 0.0$ . The corresponding initial setup in one dimension is a strong detonation. This problem is solved on  $[0, 300] \times [0, 50]$  with a

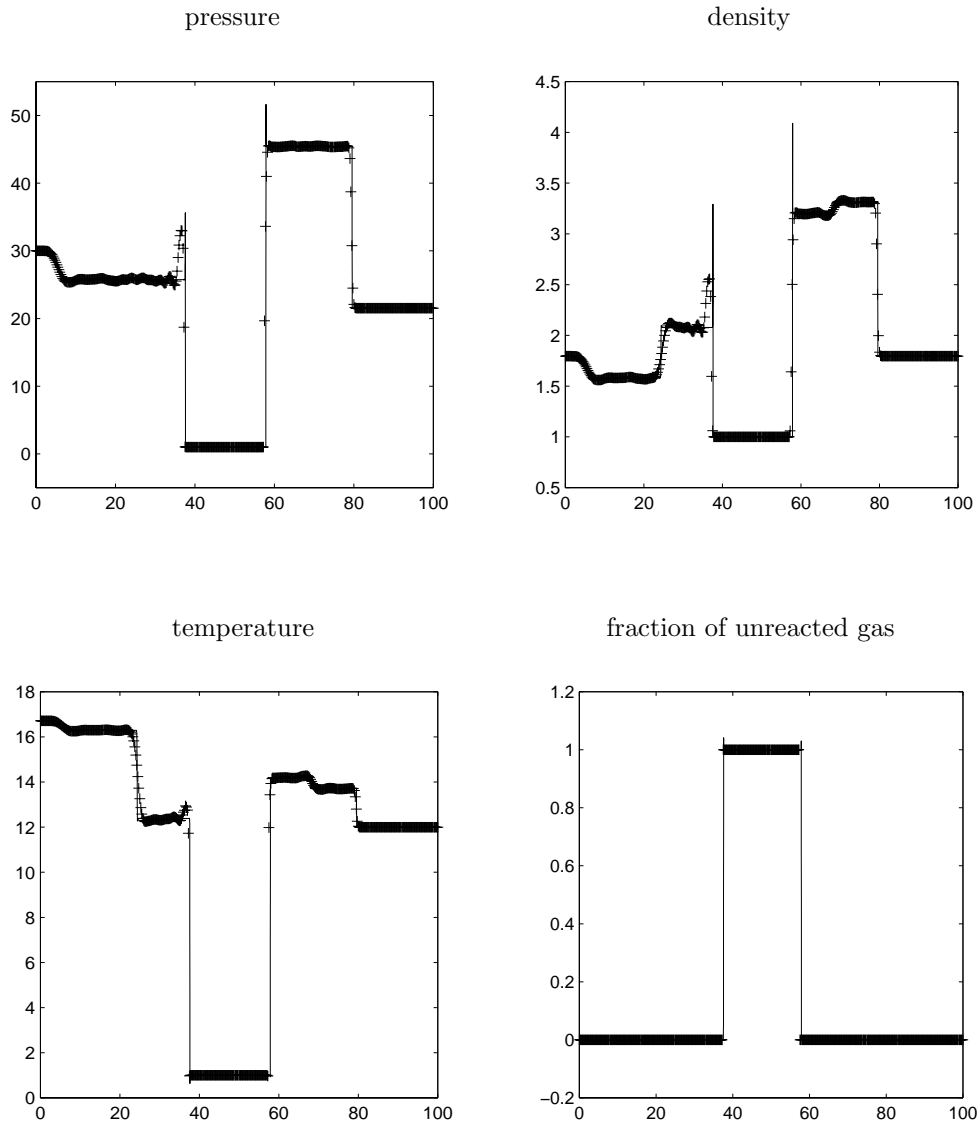


FIG. 4.6. Numerical results of Example 4.6 involving the collision of two detonations by the random projection method (2.15).  $h = 0.25$ ,  $k = 0.01$ . -: “exact” solutions; ++: computed solutions. (a) at  $t = 4$  (before collision).

$301 \times 51$  mesh, and

$$\xi(y) = \begin{cases} 10, & |y - 25| \geq 15, \\ 25 - |y - 25|, & |y - 25| < 15. \end{cases}$$

Thus the mesh size  $h = 1$ . The time step is chosen as  $k = 0.01$ .

Figure 4.7 shows density contours at several different times. One can see that the triple points, which are the important features of the solution, travel in the transverse direction and bounce back and forth against the upper and lower walls. On the con-

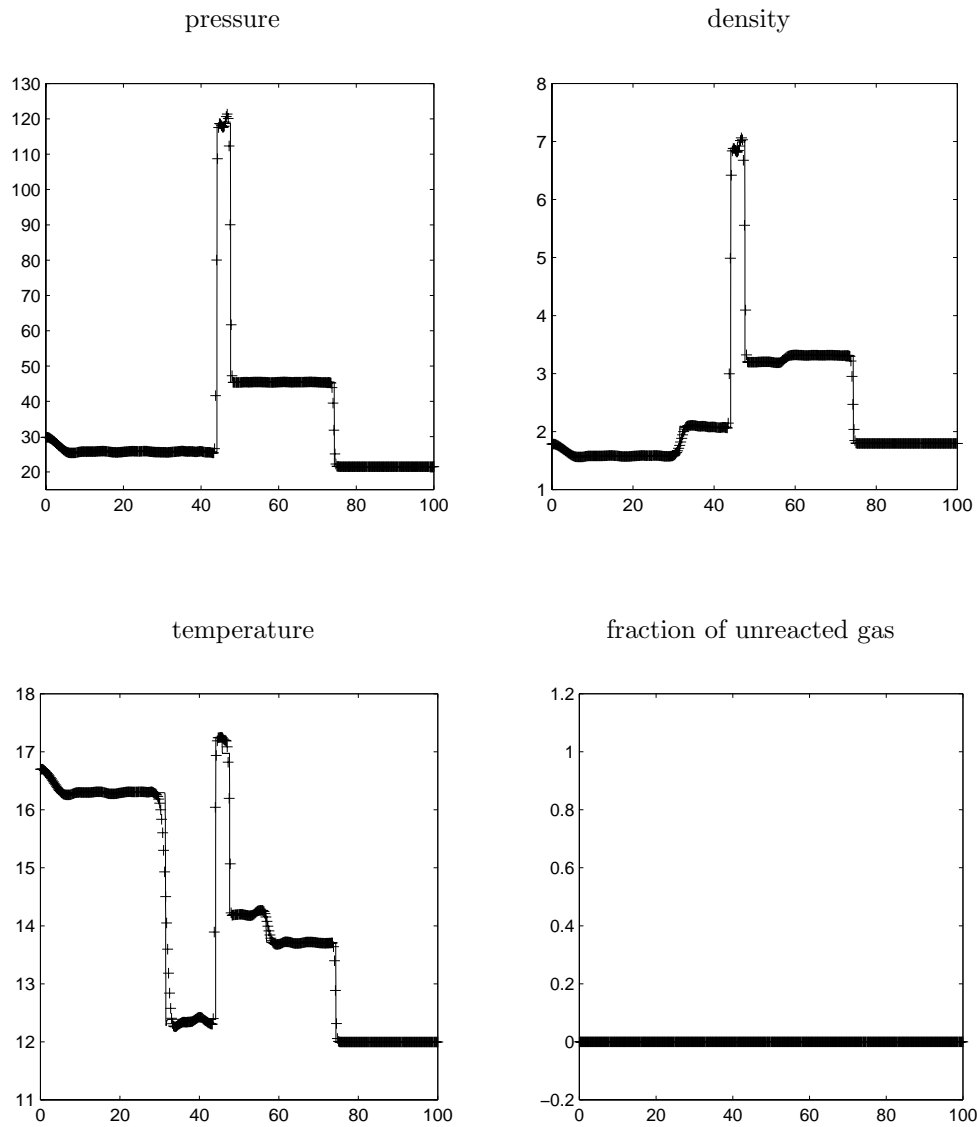


FIG. 4.6 (cont.). (b) at  $t = 6$ . After collision the detonation becomes extinct and the gas is completely burned.

trary, the triple points cease to move after some time by using the usual deterministic method [11].

*Example 4.8* (another two-dimensional detonation wave). This is a two-dimensional example with radial symmetry. The parameters are chosen as

$$\gamma = 1.2, \quad q_0 = 50, \quad K = \frac{1}{\varepsilon} = 1000, \quad \text{and} \quad T_c = 2.0.$$

A similar example was used in [15].

The initial values consist of totally burnt gas inside of a circle with radius 10 and totally unburnt gas everywhere outside of the circle. Furthermore, the unburnt and burnt states are chosen in a way analogous to the one-dimensional case, i.e.,

$$(\rho, u, v, p, z)(x, y, 0) = \begin{cases} (\rho_l, u_l(x, y), v_l(x, y), p_l, 0) & \text{if } r \leq 10, \\ (\rho_r, u_r, v_r, p_r, 1) & \text{if } r > 10, \end{cases}$$

where  $r = \sqrt{x^2 + y^2}$ ;  $p_l = 21.53134$ ,  $\rho_l = 1.79463$ ,  $u_l(x, y) = 10x/r$ ,  $v_l(x, y) = 10y/r$ ; and  $p_r = 1.0$ ,  $\rho_r = 1.0$ ,  $u_r = 0.0$ ,  $v_r = 0.0$ .

This is a radially symmetric problem, and the important feature is that the detonation front is circular. This problem is solved on the domain  $[-50, 50] \times [0, 50]$  with mesh size  $h = 0.5$  and time step  $k = 0.01$ . Solid wall boundary conditions are used along  $x = 0$ . Inflow boundary condition is used along  $x = -50$ . Outflow boundary conditions are used along  $x = 50$  and  $y = 50$ .

The random projection algorithm for this example is as follows. Notice that at any time step  $t = t_n$ , for each  $j$ , there are two integers,  $l_j(n) = l_n$  and  $r_j(n) = r_n$ , such that  $l_n \leq r_n$  and

$$(4.1) \quad z_{i,j}^n = \begin{cases} 1 & \text{if } j \leq l_j(n), \\ 0 & \text{if } l_j(n) < j < r_j(n), \\ 1 & \text{if } i \geq r_j(n). \end{cases}$$

Here  $l_j(n)$  and  $r_j(n)$  are the left and right locations of the jump for  $z$  at the grid line  $y = y_j$  in the approximate solution at time  $t_n = nk$ . Then the random project algorithm to find  $z^{n+1}$  is as follows:

$$(4.2) \quad \begin{aligned} &\tilde{S}_{2p}(k) : \text{ For } j \text{ do} \\ &\quad \text{Set } l_j(n+1) := l_j(n) + 1, \\ &\quad \text{For } l = l_j(n) + 1, l_j(n), \dots, l_j(n) - d, \text{ do} \\ &\quad \quad l_j(n+1) := l \quad \text{if } T_{l,j}^{n+1} > \theta_n, \\ &\quad \text{Set } r_j(n+1) := r_j(n) - 1, \\ &\quad \text{For } r = r_j(n) + 1, r_j(n), \dots, r_j(n) + d, \text{ do} \\ &\quad \quad r_j(n+1) := r \quad \text{if } T_{r,j}^{n+1} > \theta_n, \\ &\quad \text{If } l_j(n+1) > r_j(n+1) \text{ then} \\ &\quad \quad l_j(n+1) := r_j(n+1) := (l_j(n+1) + r_j(n+1))/2, \\ &\quad z_{i,j}^{n+1} = \begin{cases} 1 & \text{if } i \leq l_j(n+1) \\ 0 & \text{if } l_j(n+1) < i < r_j(n+1) \\ 1 & \text{if } i \geq r_j(n+1) \end{cases} \quad \text{for all } i. \end{aligned}$$

The stability condition for this algorithm is still the usual CFL condition determined from the convection step.

Figure 4.8(a) shows the velocity fields and Figure 4.8(b) shows profiles of the pressure  $p$ , temperature  $T$ , and 30 times the mass fraction of unburnt gas,  $30z$  (here we show  $30z$ , not  $z$  itself, for better visualization), on the line  $y = x$  ( $0.0 \leq x \leq 50$ ) by the random projection method (4.2) at time  $t = 1$ ,  $t = 2$ ,  $t = 4$ , and  $t = 5$ , respectively.

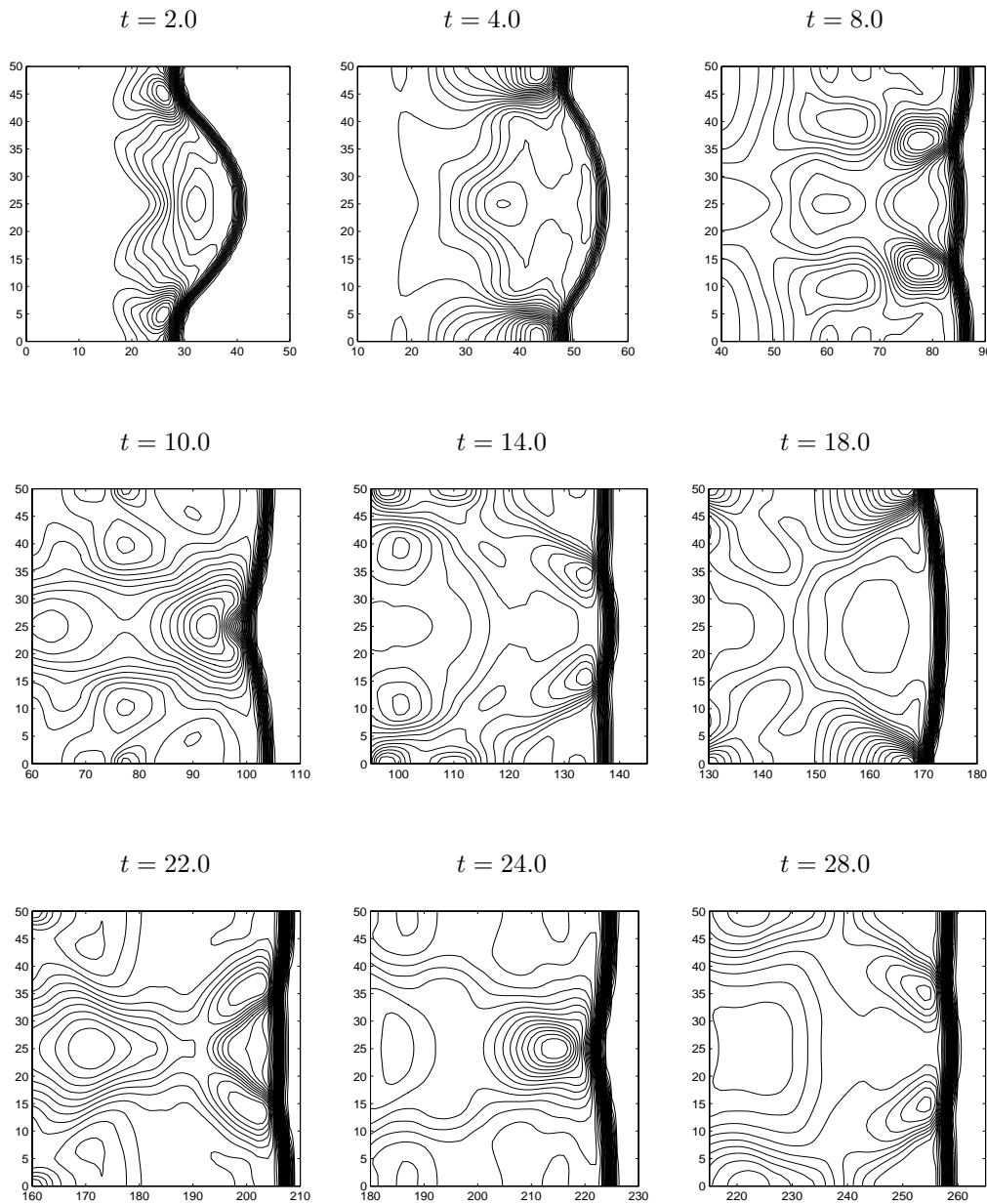


FIG. 4.7. Numerical density contours for Example 4.7 by the two-dimensional random projection method (3.4).  $h = 1.0$ ,  $k = 0.01$ .

It can be seen that the detonation front remains circular, and no spurious non-physical wave is generated when using the random projection method (4.2). On the other hand, if one uses the deterministic method, the detonation front does not remain circular, and spurious nonphysical wave is generated if the same grid size and time step are used.

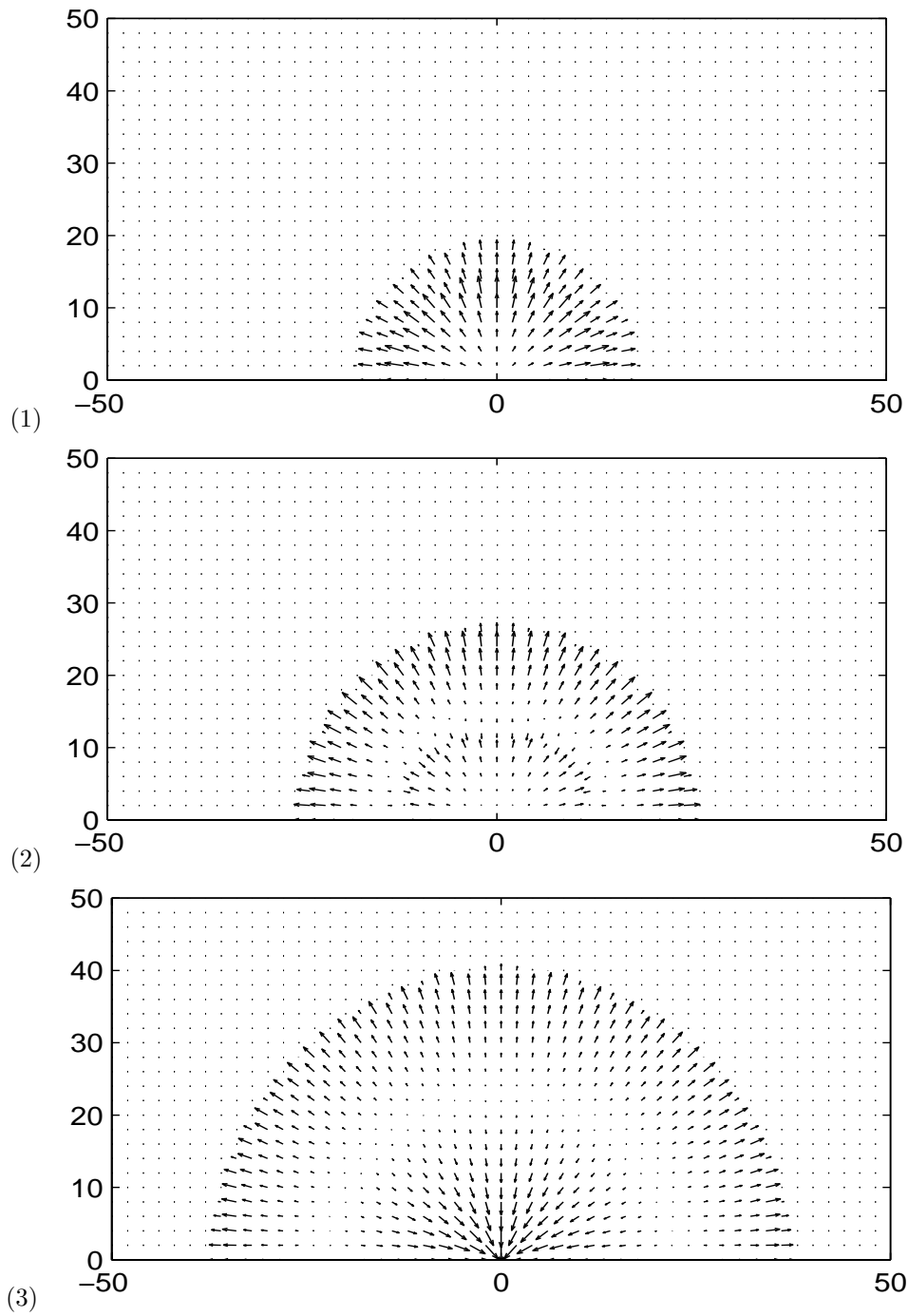


FIG. 4.8. Numerical solutions of Example 4.8 calculated by the two-dimensional random projection method (4.2) with  $h = 0.5$ ,  $k = 0.01$ . (1):  $t = 1.0$ , (2):  $t = 2.0$ , (3):  $t = 4.0$ . (a) Velocity fields at different times.



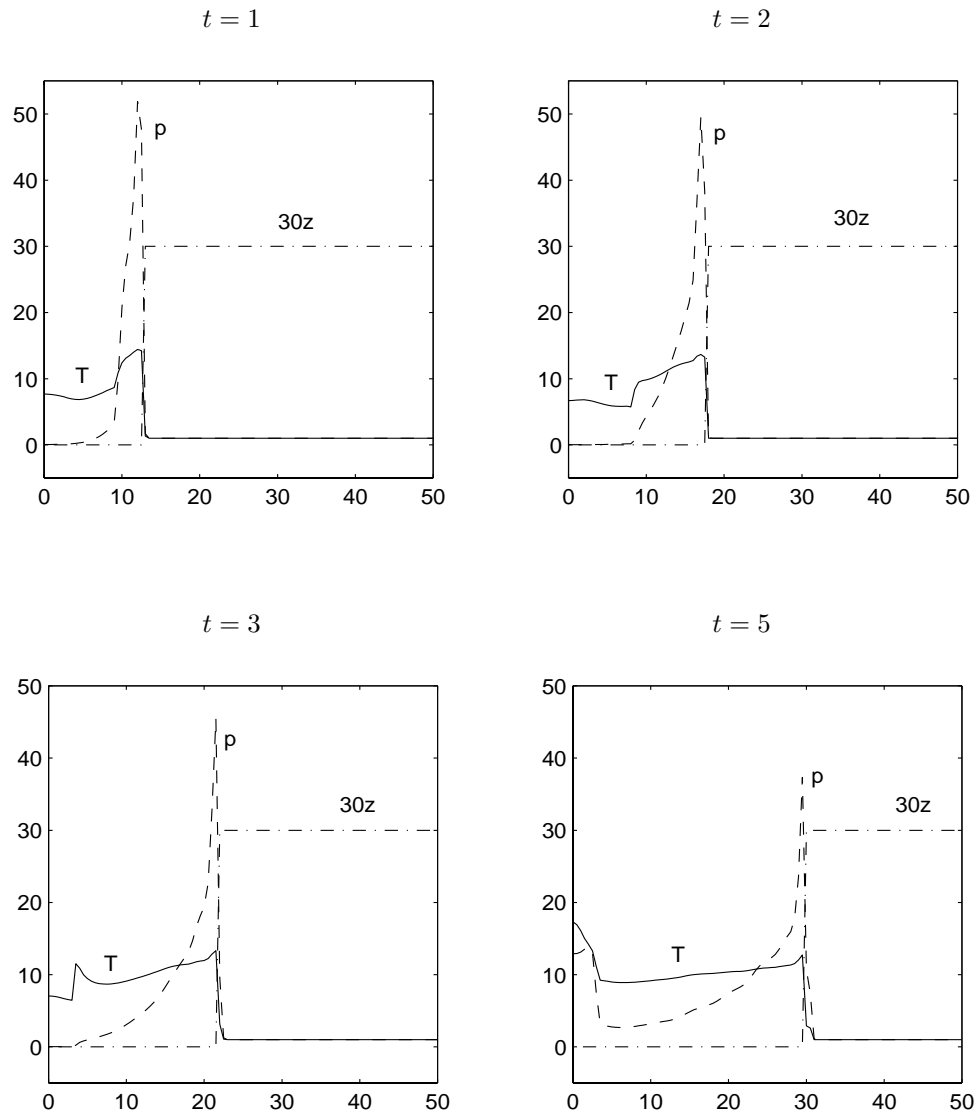


FIG. 4.8 (cont.). (b) Profiles of pressure  $p$  ( - - ), temperature  $T$  ( - ), and the fraction of unburnt gas multiplied by 30,  $30z$  ( - · ) on the line  $y = x$  ( $0 \leq x \leq 50$ ) at different times.

**5. Conclusions.** In this paper we presented a simple and robust random projection method for underresolved numerical simulation of stiff detonation waves in chemically reacting flows. This method is based on the random projection method proposed by the authors for general hyperbolic systems with stiff reaction terms [1], where the ignition temperature is randomized in a suitable domain. The method is simplified using the equations of instantaneous reaction and then extended to handle the interactions of detonations. Extensive numerical experiments, including interaction of detonation waves, and in two dimensions, demonstrate that this method, although very simple and efficient, is very reliable and robust in calculating a wide range of problems in reacting flows.

In [3] this method is generalized to multispecies reactions.

**Acknowledgments.** W. Bao thanks the School of Mathematics of the Georgia Institute of Technology and the Department of Mathematics of the University of Wisconsin-Madison for their hospitality during his extended visits there.

#### REFERENCES

- [1] W. BAO AND S. JIN, *The random projection method for hyperbolic conservation laws with stiff reaction terms*, J. Comput. Phys., 163 (2000), pp. 216–248.
- [2] W. BAO AND S. JIN, *Error Estimates on the Random Projection Methods for Hyperbolic Conservation Laws with Stiff Reaction Terms*, unpublished notes, 1999.
- [3] W. BAO AND S. JIN, *The Random Projection Method for Stiff Multi-Species Detonation Capturing*, preprint, 2000.
- [4] M. BEN-ARTZI, *The generalized Riemann problem for reactive flows*, J. Comput. Phys., 81 (1989), pp. 70–101.
- [5] A. C. BERKENBOSCH, E. F. KAASSCHIETER, AND R. KLEIN, *Detonation capturing for stiff combustion chemistry*, Combust. Theory Model., 2 (1998), pp. 313–348.
- [6] A. BOURLIOUX, A. J. MAJDA, AND V. ROYTBURD, *Theoretical and numerical structure for unstable one-dimensional detonations*, SIAM J. Appl. Math., 51 (1991), pp. 303–343.
- [7] A. J. CHORIN, *Random choice methods with applications to reacting gas flow*, J. Comput. Phys., 25 (1977), pp. 253–272.
- [8] P. COLELLA, *Glimm’s method for gas dynamics*, SIAM J. Sci. Statist. Comput., 3 (1982), pp. 76–110.
- [9] P. COLELLA, A. MAJDA, AND V. ROYTBURD, *Theoretical and numerical structure for reacting shock waves*, SIAM J. Sci. Statist. Comput., 7 (1986), pp. 1059–1080.
- [10] R. COURANT AND K. O. FRIEDRICHS, *Supersonic Flow and Shock Waves*, Interscience, New York, 1967.
- [11] B. ENGQUIST AND B. SJOGREEN, *Robust Difference Approximations of Stiff Inviscid Detonation Waves*, UCLA CAM Report 91-03, University of California-Los Angeles, Los Angeles, CA, 1991.
- [12] J. GLIMM, *Solutions in the large for nonlinear hyperbolic systems of equations*, Comm. Pure Appl. Math., 18 (1965), pp. 697–715.
- [13] D. F. GRIFFITHS, A. M. STUART, AND H. C. YEE, *Numerical wave propagation in an advection equation with a nonlinear source term*, SIAM J. Numer. Anal., 29 (1992), pp. 1244–1260.
- [14] J. M. HAMMERSLEY AND D. C. HANDSCOMB, *Monte Carlo Methods*, Methuen, London, 1965.
- [15] C. HELZEL, R. J. LEVEQUE, AND G. WARNECKE, *A modified fractional step method for the accurate approximation of detonation waves*, SIAM J. Sci. Comput., 22 (2000), pp. 1489–1510.
- [16] P. HWANG, R. P. FEDKIW, B. MERRIMAN, A. K. KARAGOZIAN, AND S. J. OSHER, *Numerical resolution of pulsating detonation waves*, Combust. Theory Model., 4 (2000), pp. 217–240.
- [17] S. JIN AND Z. P. XIN, *The relaxation schemes for systems of conservation laws in arbitrary space dimensions*, Comm. Pure Appl. Math., 48 (1995), pp. 235–276.

- [18] R. J. LEVEQUE AND H. C. YEE, *A study of numerical methods for hyperbolic conservation laws with stiff source terms*, J. Comput. Phys., 86 (1990), pp. 187–210.
- [19] R. B. PEMBER, *Numerical methods for hyperbolic conservation laws with stiff relaxation I. Spurious solutions*, SIAM J. Appl. Math., 53 (1993), pp. 1293–1330.
- [20] M. A. SUSSMAN, *Source Term Evaluation for Combustion Modeling*, AIAA paper 93-0239, 1993.
- [21] F. A. WILLIAMS, *Combustion Theory*, Addison-Wesley, Reading, MA, 1965.